Neuron, Vol. 38, 47–59, April 10, 2003, Copyright ©2003 by Cell Press

Conservation of Chloride Channel Structure Revealed by an Inhibitor Binding Site in ClC-1

Raúl Estévez,[1,3] Björn C. Schroeder,[1,3,4] Alessio Accardi,[2,5] Thomas J. Jentsch,[1,*] and Michael Pusch[1,2,*]
[1]Zentrum für Molekulare Neurobiologie Hamburg, ZMNH
Universität Hamburg
Falkenried 94
D-20246 Hamburg
Germany
[2]Istituto di Biofisica
Via de Marini 6
I-16149 Genova
Italy

Summary

Crystal structures of bacterial CLC proteins were solved recently, but it is unclear to which level of detail they can be extrapolated to mammalian chloride channels. Exploiting the difference in inhibition by 9-anthracene carboxylic acid (9-AC) between ClC-0, -1, and -2, we identified a serine between helices O and P as crucial for 9-AC binding. Mutagenesis based on the crystal structure identified further residues affecting inhibitor binding. They surround a partially hydrophobic pocket close to the chloride binding site that is accessible from the cytoplasm, consistent with the observed intracellular block by 9-AC. Mutations in presumably Cl^--coordinating residues yield additional insights into the structure and function of ClC-1. Our work shows that the structure of bacterial CLCs can be extrapolated with fidelity to mammalian Cl^- channels.

Introduction

CLC chloride channels form a large gene family that is present in all phylae (Jentsch et al., 2002). Structurally, CLC channels are unrelated to other ion channel families. Single-channel analysis and mutagenesis provided evidence for a double-barreled model (Bauer et al., 1991; Ludewig et al., 1996; Middleton et al., 1996; Miller and White, 1984) of the *Torpedo* channel ClC-0 (Jentsch et al., 1990). Indeed, the recent crystal structure analysis of bacterial CLC channels (Dutzler et al., 2002) showed a dimer with two pores. As predicted by previous mutagenesis studies (Ludewig et al., 1996; Weinreich and Jentsch, 2001), each pore is entirely contained within a single subunit of the dimer. Thus, the dimeric, double-barreled architecture is almost certainly a general feature of all CLC channels.

*Correspondence: jentsch@zmnh.uni-hamburg.de (T.J.J.), pusch@icb.ge.cnr.it (M.P.)
[3]These authors contributed equally to this work.
[4]Present address: Howard Hughes Medical Institute, University of California, San Francisco, San Francisco, California 94143.
[5]Present address: Department of Biochemistry, Howard Hughes Medical Institute, Brandeis University, Waltham, Massachusetts 02454.

Pores of CLC channels are not formed by a symmetrical assembly of homologous subunits. Hence there is no single stretch that could be termed the pore region like the P loop of voltage-gated cation channels. The structures of bacterial CLC proteins revealed an amazingly complex topology in which 18 α helices per subunit are embedded in the membrane (Dutzler et al., 2002). Most of these helices are severely tilted. Several helices do not entirely cross the membrane but extend toward the center of the membrane, where the amino acid chain turns and folds to another helix that extends back to the same side. Side chains and peptide backbones of residues at the end of such helices, which are electrically polarized, coordinate a chloride ion at its binding site in a conformation that most likely represents a closed state of the channel (Dutzler et al., 2002). A glutamate residue that is located close to the Cl^- binding site (Glu 148 of *Salmonella typhimurium* ClC [StClC]) would impede current flow through the bacterial channel, suggesting that it may have a role in gating. In agreement with these structural predictions, several regions of CLC proteins influence pore properties like ion selectivity and single channel conductance as well as gating (Estévez and Jentsch, 2002; Fahlke et al., 1995, 1997a; Ludewig et al., 1996; Pusch et al., 1995a, 1995b; Wollnik et al., 1997).

Based on homology, the nine different CLC channels of mammals can be grouped into three branches (Jentsch et al., 2002). Members of the first branch (ClC-1, -2, -Ka, and -Kb) are expressed in the plasma membrane, where they influence electrical excitability or function in transepithelial transport. Members of the other two branches (ClC-3 to -5 and ClC-6 and -7, respectively) reside predominantly in intracellular organelles (Günther et al., 1998; Kornak et al., 2001; Stobrawa et al., 2001) but may be inserted into the plasma membrane under some circumstances (Kornak et al., 2001). They play a role in acidifying intra- and extracellular compartments by shunting the current of the H^+-ATPase.

Mutations in four CLC genes are known to cause inherited human diseases: myotonia (ClC-1), Bartter's syndrome (ClC-Kb), Dent's disease (ClC-5), and osteopetrosis (ClC-7) (Koch et al., 1992; Kornak et al., 2001; Lloyd et al., 1996; Simon et al., 1997). Mutations in barttin, a β subunit of ClC-K channels, cause Bartter's syndrome with deafness (Birkenhäger et al., 2001; Estévez et al., 2001). The disruption of three other CLC genes caused severe phenotypes in mice. ClC-$2^{-/-}$ mice are blind and males infertile (Bösl et al., 2001), ClC-$3^{-/-}$ mice suffer from hippocampal and retinal degeneration (Stobrawa et al., 2001), and ClC-$K1^{-/-}$ mice have symptoms resembling diabetes insipidus (Matsumura et al., 1999). This demonstrates the physiological importance of CLC channels and suggests potential uses as drug targets. For instance, inhibitors of ClC-7 might be beneficial in osteoporosis (Kornak et al., 2001). However, the pharmacology of CLC channels is poorly developed, and nearly nothing is known about inhibitor binding sites.

In addition to their potential medical importance,

blockers or activators of ion channels are useful tools to investigate the structure-function relationship of ion channels (Hille, 2001). Known Cl^- channel inhibitors are mostly large organic anions. Several such compounds are known to inhibit members of the CLC family, but they largely lack high affinity and specificity. Two structurally unrelated classes of molecules inhibit the muscle channel ClC-1 with a relatively high potency. 9-anthracene-carboxylic acid (9-AC) blocks the macroscopic skeletal muscle Cl^- conductance (Bryant and Morales-Aguilera, 1971; Palade and Barchi, 1977). It rather potently inhibits ClC-1 (Astill et al., 1996; Steinmeyer et al., 1991) ($K_d \sim 10$ μM) but only weakly affects ClC-0 (Steinmeyer et al., 1991), ClC-2 (Clark et al., 1998), or ClC-5 (Steinmeyer et al., 1995). Because 9-AC is membrane permeable, it is currently unknown whether it directly affects the channel from the extra- or the intracellular side. Consistent with known myotonic side effects of clofibrate (Langer and Levy, 1968), clofibric acid and related substances also inhibit skeletal muscle Cl^- conductance (De Luca et al., 1992). They block ClC-0, ClC-2, and ClC-5 less potently than ClC-1 (Pusch et al., 2000). These inhibitors act from the intracellular side (Pusch et al., 2000), and their effectiveness depends on the Cl^- concentration (Pusch et al., 2001). The voltage dependence of their blocking effect (Aromataris et al., 1999) is mainly due to a state-dependent binding, with closed channels having a much higher affinity than channels in the open configuration (Pusch et al., 2001).

So far, the sites where these inhibitors bind to the channel protein have been unknown. Using a chimeric strategy that exploits the difference in inhibitor sensitivity between ClC-1 and ClC-2, we have now identified serine 537 of ClC-1 as a residue that largely determines its higher sensitivity for 9-AC and clofibrates. In the crystallized bacterial CLCs (Dutzler et al., 2002), the corresponding residue is located close to the chloride binding site. Guided by the crystal structure of the CLC protein, we identified additional residues that are important for 9-AC binding and that are located in different areas of the primary sequence. Our work suggests that a partially hydrophobic binding pocket for inhibitors is accessible from the cytoplasm and is adjacent to and possibly partially overlapping with the Cl^- binding site as revealed in the crystal of StClC. Additionally, the biophysical analysis of mutants affecting Cl^--coordinating residues gives new insights into the permeation and gating properties of CLC channels.

Results

Narrowing Down an Inhibitor Binding Site in a Chimeric Strategy

We first compared the effect of 9-AC (Figure 1A) on ClC-0, ClC-1, and ClC-$2_{\Delta 16\text{-}61}$ expressed in *Xenopus* oocytes. For experimental convenience, we used the amino-terminal deletion mutant ClC-$2_{\Delta 16\text{-}61}$ rather than wild-type (WT) ClC-2. In the *Xenopus* oocyte expression system, this deletion abolishes the slow, hyperpolarization-activated gating of ClC-2 without altering its open channel properties (Gründer et al., 1992). While ClC-1 was almost completely blocked by 100 μM 9-AC (Figure 1D), both ClC-0 and the ClC-2 mutant were only very weakly affected (Figures 1C and 1E).

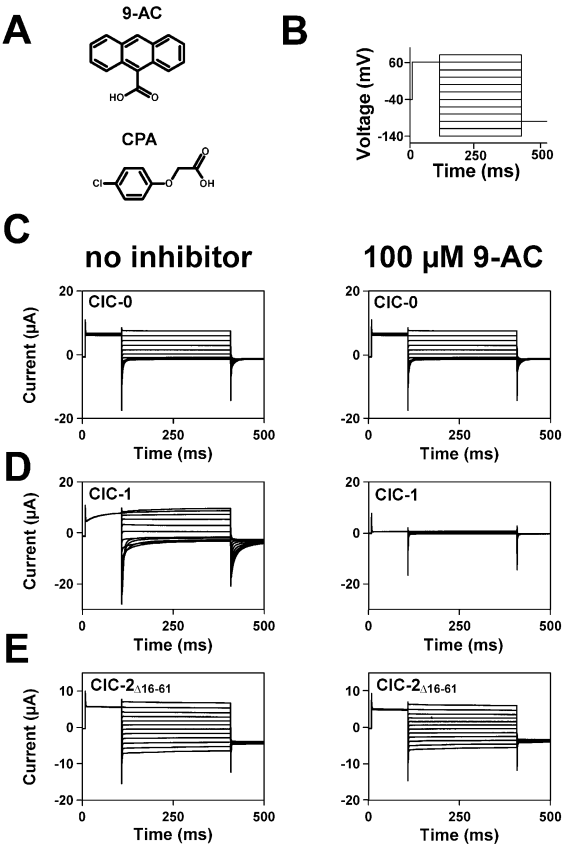

Figure 1. Inhibitor Sensitivities of Plasma Membrane CLC Channels

(A) Molecular structure of 9-anthracene-carboxylic acid (9-AC) (top), and the structurally unrelated clofibric acid derivative 4-chloro-phenoxy-acetic acid (CPA) (below). The more lipophilic 9-AC is more membrane permeable than CPA.

(B) Voltage protocol used for experiments shown in panels (C)–(E). From a holding potential of −40mV, the voltage was stepped to +60mV, followed by voltages between +80mV and −140mV (in decrements of −20mV), and a constant "tail" pulse of −100mV.

(C–E) Effect of 100 μM 9-AC on currents from ClC-0, ClC-1, and ClC-$2_{\Delta 16\text{-}61}$. Typical voltage clamp traces of *Xenopus* oocytes injected with ClC-0 (C), ClC-1 (D), and ClC$2_{\Delta 16\text{-}61}$ (E) cRNA are shown. Currents before (left) and after 3 min of continuous perfusion with 100 μM 9-AC (right) are displayed. In contrast to ClC-1, whose current was blocked by more than 90%, ClC-$2_{\Delta 16\text{-}61}$ and ClC-0 were nearly unaffected by this concentration of 9-AC.

We subsequently constructed chimeras between ClC-$2_{\Delta 16\text{-}61}$ and ClC-1 to identify structural determinants of 9-AC binding (Figure 2A). They yielded large, albeit altered currents upon heterologous expression (data not shown). Unfortunately, the current block by 9-AC and its washout were very slow, with steady-state inhibition for some mutations of ClC-1 not being reached even after 20 min (see Figure 2D). As we were interested in large differences of 9-AC potency, we therefore determined apparent K_ds semiquantitatively as described in Experimental Procedures. This yielded an apparent K_d of 13 $\pm$ 2 μM (Figure 3D) (at −40mV) for ClC-1, in good agreement with previously reported values for the macroscopic Cl^- conductance of muscle (11 μM [Palade and Barchi, 1977]) and for heterologously expressed ClC-1 (7 μM [Astill et al., 1996]). For ClC-$2_{\Delta 16\text{-}61}$, the corre-

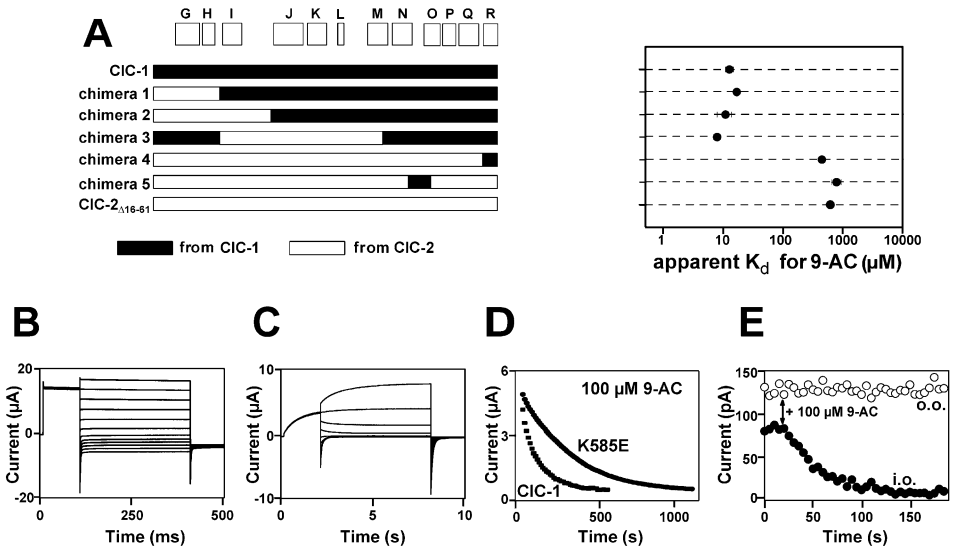

Figure 2. Chimeric Strategy to Narrow Down the ClC-1 9-AC Binding Site

(A) Schematic diagram showing the constructions of chimera 1 (ClC-$2_{\Delta 16\text{-}61;\leq 273}$;ClC-$1_{\geq 295}$), 2 (ClC-$2_{\Delta 16\text{-}61;\leq 322}$;ClC-$1_{\geq 344}$), 3 (ClC-$1_{\leq 295}$;ClC-$2_{\geq 273;\leq 449}$;ClC-$1_{\geq 468}$), 4 (ClC-$2_{\Delta 16\text{-}61;\leq 554}$;ClC-$1_{\geq 574}$), and 5 (ClC-$2_{\Delta 16\text{-}61;\leq 477}$;ClC-$1_{\geq 498;\leq 528}$;ClC-$2_{\geq 513}$) and corresponding apparent K_d values for 9-AC inhibition (right). For clarity, the amino- and carboxyterminal ends of the proteins are not shown. The localization of protein helices G-R (deduced from the bacterial structure) are shown above the left diagram. The channels fall into a "high-affinity class" that includes ClC-1 and chimeras 1, 2, and 3; and a "low-affinity class" that includes ClC-$2_{\Delta 16\text{-}61}$ and chimeras 4 and 5. Apparent K_ds (at −40mV) were averaged from 5 to 10 experiments.

(B) Typical voltage clamp traces of chimera 1 with voltage protocol as in Figure 1B.

(C) Voltage clamp trace of chimera 1 after application of 1 mM 9-AC. From the holding potential of −40mV, voltage was stepped to +60mV for 2 s, followed by test potentials between +80mV and −140mV (duration 6 s, in −20mV decrements), and a constant "tail" pulse of −100mV (2 s). Note the different time scale and the slow current relaxations that are compatible with a slow voltage-dependent inhibition from the inside. The time-dependent activation at positive voltages is due to an unbinding of 9-AC that is much faster than inhibitor kinetics with WT ClC-1 (Figure 1D) and that results in larger currents for the chimera under these conditions.

(D) Onset of inhibition by 9-AC of ClC-1 and its mutant K585E. In two-electrode voltage clamp, a 100 ms test pulse to +60mV was applied every 12 s to monitor the development of inhibition by 100 μM 9-AC that was applied briefly before the first pulse shown in the graph and remained in the bath. The current at the end of the 60mV pulse is plotted versus time (lower line, ClC-1; upper line, K585E) for representative oocytes. Exponential fits yielded time constants of 142 ± 29 s (n = 5) and 774 ± 308 s (n = 3) for ClC-1 and K585E, respectively.

(E) Effect of 100 μM 9-AC on ClC-1 in inside-out (filled circles) and outside-out (open circles) patches held at 0mV and stepped repeatedly every 5 s to +80mV and −140mV. The absolute steady-state current at −140mV is plotted as a function of time. 100 μM 9-AC was applied at the time point indicated by the arrow.

sponding value was about 50-fold larger (K_d = 620 ± 66 μM). Apparent K_ds of chimeras 1, 2, and 3 were close to the one of ClC-1, while K_ds of chimeras 4 and 5 resembled the one of ClC-$2_{\Delta 16\text{-}61}$ (Figure 2A). These results suggest that the difference in potency of 9-AC is determined by the region encompassing helices M through Q and that the hydrophilic N-O linker is unlikely to be involved.

9-AC Block Is Voltage Dependent and It Acts from the Intracellular Side

Chimera 1 gave additional insights into the mechanism of 9-AC binding. In the presence of 1 mM 9-AC (Figure 2C) but not in its absence (Figure 2B), currents increased slowly (within seconds) upon depolarization. They decreased with a similar time course upon hyperpolarization. This might be explained by a slow, voltage-dependent inhibitor binding in the inner opening of the pore: upon rendering the cells inside-positive, the negatively charged 9-AC would be driven out of the pore. However, similar to observations made with the clofibrate block of ClC-0 (Pusch et al. 2001), a state-dependent binding of 9-AC may also contribute to the observed voltage dependence.

A more efficient block at negative voltages was observed with WT ClC-1 as well. However, very long pulses (>60 s in inside-out patch clamp measurements) were needed to detect this voltage dependence (data not shown). This slow kinetics might explain why this voltage dependence has escaped the attention of other investigators.

The positive charge of the lysine 585 (ClC-1) seems to control the cytoplasmic access of Cl^- to the pore by electrostatic interactions (Dutzler et al., 2002; Middleton et al., 1996; Pusch et al., 1995a). If intracellular 9-AC gains access to its binding site through the same pathway, a charge reversal of this residue should affect the kinetics but not the K_d of inhibition. Indeed, while having only minor effects on K_d (Figure 5), the K585E mutation significantly slowed the kinetics of channel block (Figure 2D). The time constant for the onset of inhibition by 100 μM 9-AC was 142 ± 29 s (n = 5) and 774 ± 308 s (n = 3) for ClC-1 and K585E, respectively.

These results strongly suggested that 9-AC binds from the intracellular side. The slow onset of inhibition

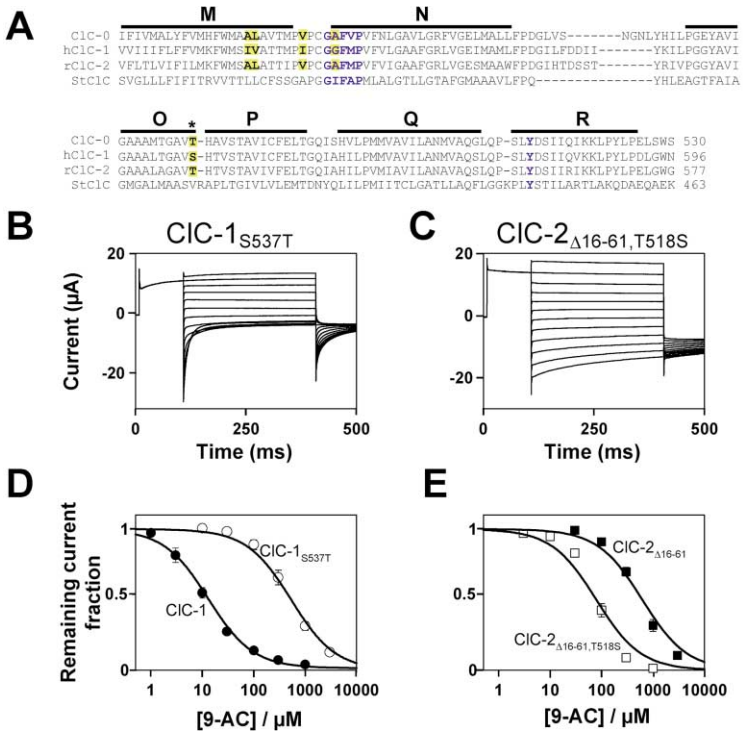

Figure 3. A Single Serine-Threonine Exchange between Helix O and P Drastically Changes 9-AC Block of ClC-1 and ClC-2

(A) Alignment of ClC-0, human ClC-1, rat ClC-2, and *Salmonella typhimurium* StClC in the region encompassing helices M to R (indicated above) that was identified in the chimeric strategy to be important for 9-AC binding to ClC-1. Amino acids in ClC-1 that differ in both ClC-0 and ClC-2 are highlighted by yellow background shading. The S537 residue of ClC-1 is indicated by an asterisk. Blue letters indicate residues involved in chloride binding as suggested by Dutzler et al. (2002). Numbers of the last amino acids are given at right.

(B) Voltage clamp traces of *Xenopus* oocytes injected with ClC-1_{S537T}, and (D) its sensitivity to 9-AC in comparison to WT ClC-1 (open and filled circles, respectively).

(C) Voltage clamp traces of ClC-$2_{\Delta16\text{-}61,T518S}$, and (E) its sensitivity to 9-AC in comparison to ClC-$2_{\Delta16\text{-}61}$ (open and filled squares, respectively).

upon extracellular application of 9-AC (Figure 2D) may therefore be caused by a slow intracellular accumulation of membrane-permeable 9-AC. To address the question of the sidedness of 9-AC binding directly, we used excised patch clamp experiments (Figure 2E). Whereas the compound had no effect in outside-out patches (open circles), it strongly inhibited ClC-1 currents in inside-out patches (filled circles). In contrast to the two-electrode voltage clamp measurements for which 9-AC inhibition was practically irreversible, washout was nearly complete within minutes in inside-out patch clamp experiments (data not shown). Furthermore, the onset of inhibition was considerably faster, with a time constant at 100 μM 9-AC of 38.3 $\pm$ 3.4 s (n = 3). Taken together, these results demonstrate that the 9-AC binding site was directly accessible from the inside only.

A Serine between Helix O and P Is Important for 9-AC Binding

The chimeric approach suggested that the region between helices M and Q might harbor structures important for 9-AC binding. In a simple situation, a difference of only one or few amino acids might account for the higher 9-AC sensitivity of ClC-1 when compared to ClC-0 or ClC-2. In such a case, the residue at the critical position is expected to differ from ClC-1 in *both* ClC-0 *and* ClC-2 because both channels are insensitive to 9-AC. Only five residues in the region encompassing helices M through Q fulfill this criterion: ClC-1 residues I472, V473, I479, G483, and S537 (Figure 3A). The corresponding amino acids in ClC-0 and ClC-2 are alanine, leucine, valine, alanine, and threonine, respectively, and are identical in both channels.

In a first step, we mutated serine 537, a residue located between helix O and P in a highly conserved region, to threonine. We also did the reverse mutation in ClC-$2_{\Delta16\text{-}61}$ (T518S). The voltage dependencies of the mutants (ClC-1_{S537T} and ClC-$2_{\Delta16\text{-}61,T518S}$) were similar to the respective WT channels (Figures 3B and 3C). Most importantly, either construct differed drastically in their inhibitor sensitivity from its WT counterpart (Figures 3D and 3E). The apparent K_d for 9-AC increased about 40-fold in ClC-1_{S537T} (from 13 $\pm$ 2 μM [n = 10] to 539 $\pm$ 59 μM [n = 5]). Conversely, the K_d of ClC-$2_{\Delta16\text{-}61,T518S}$ decreased about 8-fold from 620 $\pm$ 66 μM (n = 6) to 79 $\pm$ 8 μM (n = 6). As these single amino acid exchanges largely transfer inhibitor sensitivities from ClC-1 to ClC-2 and vice versa, we conclude that this residue is a key determinant of 9-AC block.

By contrast, replacing the corresponding threonine by serine in ClC-0 proved insufficient to render it sensitive to 9-AC. Both WT ClC-0 and its T471S mutant had an apparent K_d for 9-AC that was above 1 mM (data not shown).

We subsequently changed S537 of ClC-1 to several other amino acids (Figure 5, in segment labeled "O-P"). When replaced by phenylalanine (S537F), 9-AC affinity (indicated by black bars) was further decreased by an order of magnitude in comparison to the original S537T mutant. S537C affected 9-AC block less than S537T, whereas S537A even increased 9-AC binding. The effect on 9-AC binding roughly correlated with the volume of the introduced side chains (Figure 5, inset). Also, mutations of the directly adjacent residues V536 and H538, both of which are conserved among ClC-0, ClC-1, and ClC-2, affected 9-AC block. Replacing V536 by tryptophane (V536W) drastically reduced inhibition, and the

H538K mutation significantly reduced 9-AC sensitivity as well (Figure 5).

CPA and 9-AC Binding Are Affected by the Same Serine Residue

We next used inside-out patch clamp experiments to determine whether the S537T mutation in ClC-1 also affects its sensitivity to p-chloro-phenoxy-acetic acid (CPA; Figure 1A), a derivative of clofibric acid known to inhibit this channel (Pusch et al., 2000). Both WT and mutant ClC-1 were inhibited in a voltage-dependent manner by CPA (Figures 4A and 4B). Similar to the sensitivity to 9-AC, the WT channel was >10-fold more sensitive to CPA than the S537T mutant when measured at −140mV (Figure 4G). Thus, the ClC-1 residue serine 537 influences inhibition by both 9-AC and CPA. Importantly, the ClC-$2_{\Delta 16\text{-}61,T518S}$ mutant, when compared to ClC-$2_{\Delta 16\text{-}61}$, was not only more sensitive to 9-AC, but also to CPA (Figures 4E–4G).

The C212S mutant (Lin et al., 1999) that abolishes slow gating was used in previous studies of ClC-0 inhibition (Pusch et al., 2000, 2001). Therefore, we used this background to study the block of ClC-0 by CPA. Surprisingly, the ClC-$0_{C212S,T471S}$ mutant displayed a >10-fold increase of CPA potency (at –140mV) when compared to ClC-0_{C212S} (Figures 4C, 4D, and 4G). Thus, the single serine/threonine exchange almost quantitatively "toggles" the CPA sensitivity between ClC-1 and ClC-0 but does not increase 9-AC affinity of ClC-0. Hence, the structural requirements for binding 9-AC or the chemically unrelated CPA are overlapping but not identical.

Additional Residues Involved in 9-AC Inhibition Identified by Homology to StClC

The amino acid of the *S. typhimurium* ClC (StClC) protein corresponding to serine 537 of ClC-1 is valine 402. The recently published crystal structure (Dutzler et al., 2002) revealed that this valine is close to the intracellular face of the chloride binding site, in agreement with our observation that 9-AC and CPA act from the cytoplasmic side. The side chain of V402 of StClC protrudes into a rather hydrophobic pocket that is close to the bound Cl^- (Dutzler et al., 2002) (Figure 6B). Based on homology to StClC, we selected several ClC-1 residues that surround this pocket. We also mutated several residues whose side chains protrude away from this pocket or that are relatively far away from S537. All selected amino acids were mutated to alanine and to tryptophane. Some residues were additionally mutated to other amino acids (see Figure 5 for a complete list). These mutants were tested for 9-AC sensitivity in two-electrode voltage clamp experiments in comparison to WT ClC-1 (Figure 5, black bars). Some were also tested in inside-out patch clamp experiments for their sensitivity to CPA (yellow bars).

We classified residues in three classes according to their changes in K_d values for 9-AC or CPA upon mutagenesis: "high-impact" residues (arbitrarily) defined by $|\log[K_d(\text{mutant})/K_d(\text{WT})]| \geq 1$ for at least one mutant at this position, "medium-impact" residues with $1 > |\log[K_d(\text{mutant})/K_d(\text{WT})]| \geq 0.5$, and "low-impact" ones with $|\log[K_d(\text{mutant})/K_d(\text{WT})]| < 0.5$.

High-impact residues (in red in Figure 6) were found in four well-defined regions and included the glutamate

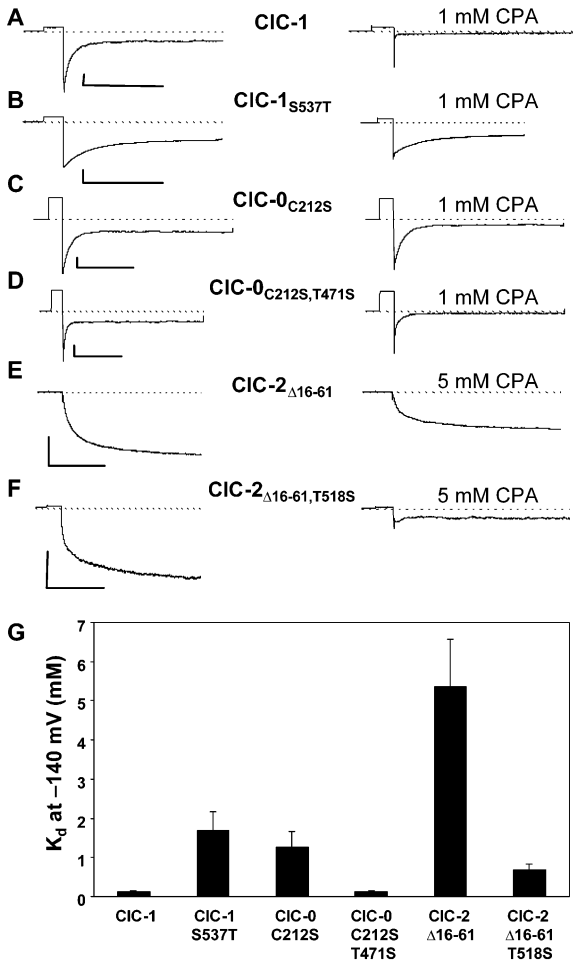

Figure 4. Effect of CPA on ClC-1, ClC-0, ClC-2, and Its Mutants

(A) Current traces of ClC-1 before (left) and after (right) application of CPA, measured in an inside-out patch. From a holding potential of 0mV, the voltage was first stepped to 60mV for 50 ms and then to −140mV. Similar experiments are shown for the ClC-1 mutant S537T (B), the ClC-0 mutant C212S (C), the ClC-0 double mutant C212S/T471S (D), ClC-$2_{\Delta 16\text{-}61}$ (E), and ClC-$2_{\Delta 16\text{-}61}$ carrying the T518S mutation (F). Holding potential in (E) and (F) was +40mV. The applied CPA concentration (1 mM for the ClC-0 and ClC-1 constructs; 5 mM for the ClC-2 constructs) matches approximately the apparent K_d at −140mV of the respective channels with a threonine at the position corresponding to 537 in ClC-1. Note that like currents from the N-terminal deletion mutant ClC-$2_{\Delta 16\text{-}61}$, ClC-$2_{\Delta 16\text{-}61,T518S}$ currents show time-dependent activation upon hyperpolarization when measured in excised patches (E and F). By contrast, they almost totally lack voltage-dependent current relaxations when examined by two-electrode voltage clamp measurements of oocytes (Figure 2C) (Gründer et al., 1992). The reason for this difference, which has been noted before (Pusch et al., 1999, 2000; Varela et al., 2002), is not clear. Horizontal scale bars in (A)–(F) indicate 200 ms, while vertical scale bars indicate 500 pA (B–E), 50 pA (A), and 200 pA (F). The dotted line indicates I = 0 throughout.

(G) The apparent K_d for CPA measured at steady state at −140mV is plotted for the indicated constructs. Error bars indicate SEM. Having a serine increases the affinity 8-fold for mutant ClC-$2_{\Delta 16\text{-}61}$, 10-fold for ClC-0_{C212S}, and 16-fold for ClC-1 compared to having a threonine at position 537 (numbering of ClC-1).

at the beginning of helix F (E232); the phenylalanine at the beginning of helix H (F288); three residues at the beginning of helix N (G483, F484, and V487); and three

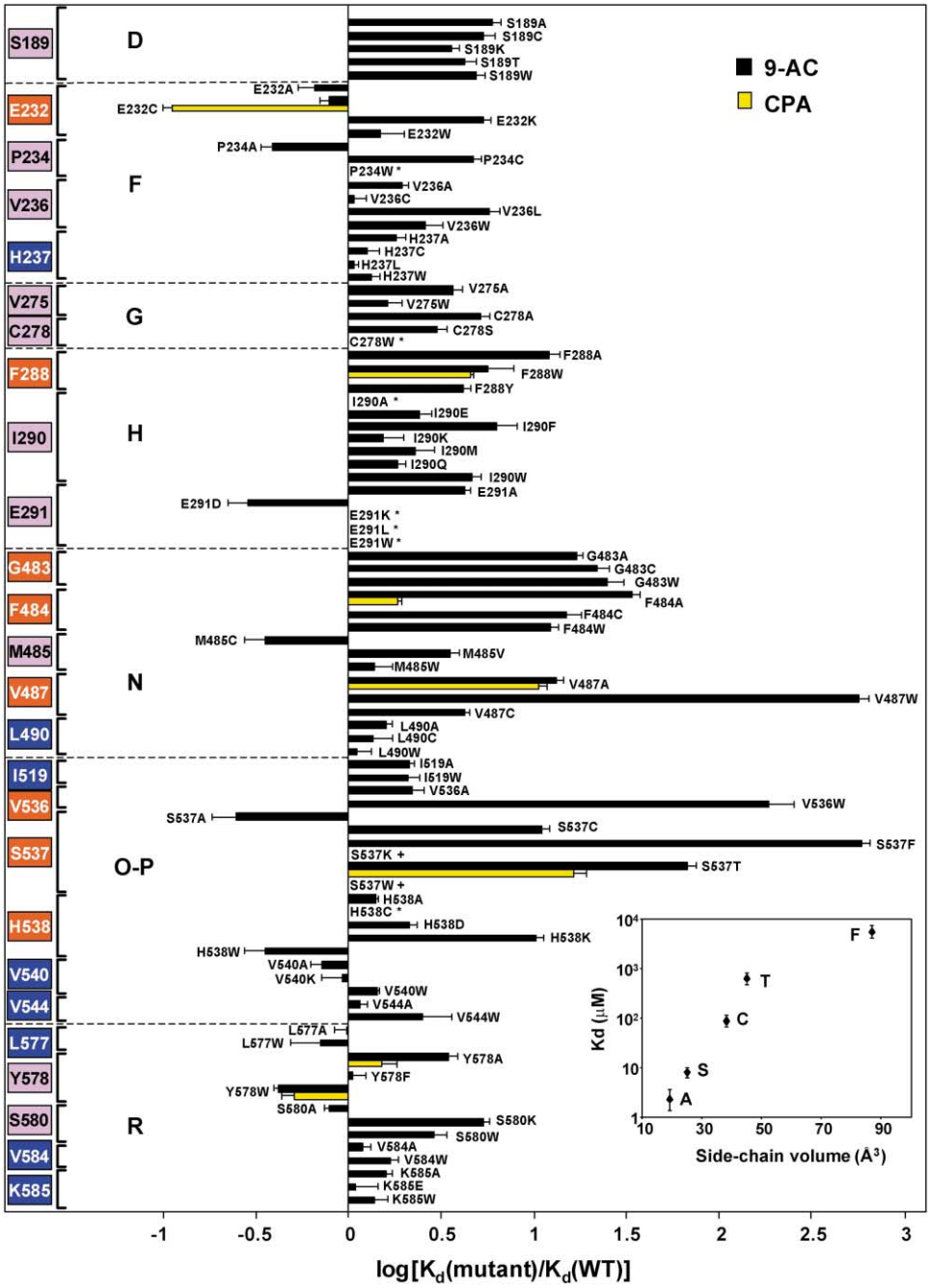

Figure 5. Effect of ClC-1 Point Mutations on the Inhibition by 9-AC and CPA

Apparent inhibitory constants (K_ds) for 9-AC (black bars, measured at −40mV) and CPA (yellow bars, measured at −140mV) for mutants of ClC-1 as determined in two-electrode voltage clamp measurements (9-AC) and inside-out patch clamp measurements (CPA) of channels expressed in *Xenopus* oocytes. These values are shown as the logarithm of ratios over the respective K_d values of WT ClC-1 ($K_d = 13 \pm 2$ μM for 9-AC and $K_d = 104 \pm 20$ μM for CPA). Error bars show SEM. The bold letters in the left part of the diagram indicate the helices where the mutated residues are located. These residues are given at left. Their importance for inhibitor binding is color coded. High-impact residues (arbitrarily defined by $|\log[K_d(\text{mutant})/K_d(\text{WT})]| \geq 1$) for at least one mutation are shown on red background, medium-impact residues ($1 > |\log[K_d(\text{mutant})/K_d(\text{WT})]| \geq 0.5$) on pink, and low-impact residues ($|\log[K_d(\text{mutant})/K_d(\text{WT})]| < 0.5$) on blue background. These colors correspond to the ones used for residues in Figure 6. Note that some amino acids that are crucial for 9-AC binding also affect the block by CPA but to quantitatively different degrees (for example, E232 and F484). Asterisks (*) indicate mutants with currents that were too small for a quantitative analysis of K_d, and mutants labeled with "+" resulted in a K_d for 9-AC that was too large to be reliably determined. Inset: K_ds for 9-AC for several substitutions at position 537 as a function of side chain volume according to Creighton (1993). When S537 was substituted by K or W, the side chains of which are equal or larger than that of F, the K_ds of the mutants were so large that they could not be measured reliably.

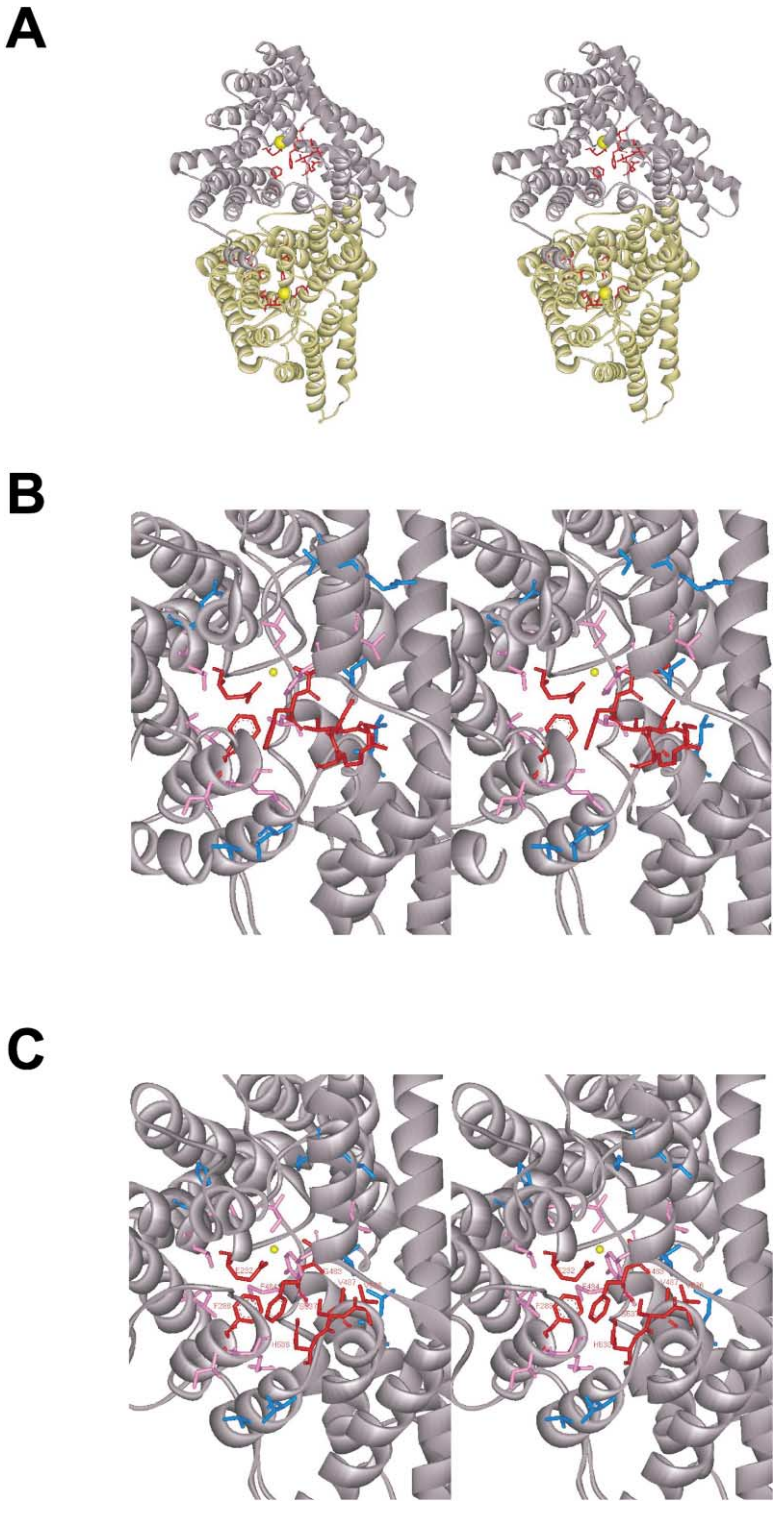

Figure 6. Three-Dimensional Representations of the Inhibitor Binding Site

(A) Stereo view of a ribbon representation of the StClC dimer (Dutzler et al., 2002). The dimer is seen from the cytoplasmic side and is slightly tilted from the symmetry axis. The chloride ions are shown as yellow balls. StClC side chains of amino acids equivalent to ClC-1 residues that had large effects on inhibitor sensitivity when mutated are shown in red (high-impact residues). These are E148 (E232), F199 (F288), I356 (G483), F357 (F484), M360 (V487), S401 (V536), V402 (S537), and R403 (H538) (in parentheses, the equivalents in ClC-1). Note that the classification of E148 (E232) as high-impact residue is based on its effect on CPA binding (Figure 5).

(B) Stereo view of the bacterial equivalent of the ClC-1 inhibitor binding pocket at higher magnification. Red marks high-impact residues as in (A). Pink color highlights amino acids that are equivalent to ClC-1 residues whose mutations had intermediate effects on channel block. These are (corresponding ClC-1 residues in parentheses) S107 (S189), P150 (P234), V152 (V236), L186 (V275), A189 (C278), I201 (I290), E202 (E291), A358 (M485), Y445 (Y578), and T447 (S580). Blue color indicates amino acids with negligible effect (low-impact residues): Q153 (H237), L363 (L490), L384 (I519), L406 (V540), L410 (V544), L444 (L577), R451 (V584), and T452 (K585).

(C) Stereo view of the inhibitor binding pocket of ClC-1 as modeled on the basis of the crystal structure of StClC (see Experimental Procedures). Color coding of residues as in (B). These residues are specified in (A) and (B), in brackets. The lower left in panel (B) displays helix A, which has not been included in the modeling of ClC-1 (C), as there is no homology in this N-terminal part.

adjacent amino acids in the region O-P (V536, S537, H538), including the serine identified in the chimeric approach. The equivalents of G483 and F484 in StClC (I356 and F357, respectively) coordinate a Cl^- ion in the StClC crystal (Dutzler et al., 2002). E232 of ClC-1 corresponds to E148 of StClC, the glutamate whose side chain may block Cl^- permeation on the extracellular side of the bound chloride. The side chains of the StClC residues that correspond to the ClC-1 residue F288 in helix H (F199) and to the high-impact residues in loop O-P, however, do not directly interact with the Cl^- ion in the crystal (Dutzler et al., 2002).

Mutations of several other amino acids resulted in intermediate effects on 9-AC affinity (shown in pink in Figure 6). Many of these medium-impact residues (e.g., P234, V236, I290, E291, M485) are close in the primary

sequence to amino acids whose mutations caused drastic changes in K_d, while others localized to different regions (e.g., S189, V275, C278, Y578, S580). Dutzler et al. (2002) have identified two amino acids (S107 at the N-terminal end of helix D and Y445 at the N terminus of helix R) that coordinate the Cl^- ion with the OH groups of their side chains. Mutating the equivalent residues (S189 and Y578, respectively) in ClC-1 had intermediate effects on 9-AC sensitivity (Figure 5). Other mutations in helix R had either intermediate (S580K) or minor (e.g., V584 or K585) effects.

As already suggested by the differential effect of the T471S mutation in ClC-0 on 9-AC and CPA block, ClC-1 mutations did not change inhibition by 9-AC or CPA strictly in parallel. For instance, S537T and in particular F484A had larger effects on inhibition by 9-AC compared to CPA, whereas F288W and V487A decreased either K_d by roughly the same factor. E232C had a strongly increased CPA affinity with the block by 9-AC being only slightly changed.

Residues that Strongly Affect Block Line a Pocket Close to the Bound Cl^- Ion

Figure 6A displays the structure of the dimeric StClC protein (Dutzler et al., 2002), with residues corresponding to ClC-1 amino acids strongly influencing 9-AC and/or CPA block being shown in red. As the image is slightly tilted from the symmetry axis, the positions of the amino acids that strongly influence inhibitor binding are shown at slightly different angles in the two subunits. These residues cluster in the region of V402 (the equivalent to ClC-1 S537) and the chloride ion (yellow) and surround a putative binding pocket, as shown in higher magnification in Figure 6B. In addition to the high-impact amino acids already shown in panel A, Figure 6B shows residues corresponding to amino acids in ClC-1 that had only intermediate effects on K_d when mutated (medium-impact residues, in pink) and those with minor effects (low-impact residues, in blue). To give an idea of the binding pocket with the relevant amino acid side chains, Figure 6C shows the same region in a homology model of ClC-1 based on the StClC structure. From these pictures it is apparent that those amino acids that strongly affected channel inhibition define a small "pocket" close to the chloride binding site. The side chains of several of these high-impact residues, most notably F288, F484, E232, S537, and H538, point into a partially hydrophobic pocket. Several of the residues with intermediate effects are close to high-impact amino acids. As with the high-impact residues mentioned above, their side chains often but not always point into this hydrophobic pocket.

In contrast, the side chains of residues with minor effects point away from this pocket or are at a relatively large distance from it. These results strongly support the notion that most or all mutations with large effects on channel block do not change inhibitor binding by nonspecific conformational rearrangements of the pore structure. It is rather inferred that these amino acids line an inhibitor binding pocket that is close to the crystallographically resolved Cl^- ion and that is accessible from the cytoplasmic side.

Creating a 9-AC Binding Site in ClC-0 in a Double Mutant

As the T471S mutation in ClC-0 increased the potency of CPA but not of 9-AC, we sought to identify additional residues whose mutations may render ClC-0 susceptible to 9-AC. Comparing the amino acid sequence of ClC-0 and ClC-1 in the vicinity of the critical S537 (ClC-1) (Figure 3A), two potentially interesting differences were identified. The two amino acids (G483 and M485) directly adjacent to F484 (ClC-1), a residue that contributes to 9-AC binding in ClC-1 (Figure 5), differ between ClC-1 and ClC-0. G483 (ClC-1) is replaced by alanine in ClC-0 but also in ClC-2, whose $ClC\text{-}2_{\Delta 16\text{-}61,T518S}$ mutant was sensitive to 9-AC. However, since the G483A mutation in ClC-1 reduced 9-AC potency (Figure 5), it seemed reasonable to test whether the reverse mutation in ClC-0 (A417G) increased 9-AC sensitivity in the background of the $ClC\text{-}0_{T471S}$ mutant. M485 is present at the equivalent position in ClC-2 but not in ClC-0, suggesting that the difference in this amino acid might explain the differential effect of 9-AC on $ClC\text{-}2_{\Delta 16\text{-}61,\ T518S}$ and $ClC\text{-}0_{T471S}$.

Whereas the block by 9-AC was not significantly changed in $ClC\text{-}0_{T471S,\ A417G}$ (data not shown), $ClC\text{-}0_{T471S,\ V419M}$ showed a dramatic increase in 9-AC sensitivity (Figure 7C) ($K_d = 107 \pm 12\ \mu M$), whereas the single mutation in $ClC\text{-}0_{T471S}$ (Figure 7A) and $ClC\text{-}0_{V419M}$ (Figure 7B) failed to confer inhibition by 9-AC ($K_d > 1$ mM). Thus, it suffices to mutate T471 to S to confer CPA binding to ClC-0, while 9-AC binding additionally requires a methionine residue at position 419 (V419M).

Biophysical Properties of Selected Mutants

As many of the mutations analyzed here affected residues that are close to the pore or even coordinate Cl^- in the StClC crystal, it was of interest whether they changed biophysical channel properties. Many of these mutations altered gating to varying degrees (Figures 8A–8F), and some changed single-channel conductance.

Noise analysis of $ClC\text{-}1_{S537T}$, a mutant with a very large effect on 9-AC binding, revealed that the single-channel conductance was not significantly different from WT (1-2 pS) (Pusch et al., 1994; Saviane et al., 1999) (data not shown). Likewise, direct single-channel analysis of the reverse *Torpedo* mutant $ClC\text{-}0_{T471S}$ showed WT conductance levels (8-10 pS; data not shown). Both mutants displayed the $Cl^- > Br^- > I^-$ selectivity of the WT. Thus, while a serine at this position is crucial for 9-AC and CPA block, it is probably not directly involved in forming the ion-selective pore.

By contrast, noise analysis of $ClC\text{-}1_{F484A}$ (Figure 8G), another mutant with significantly reduced 9-AC affinity, indicated a >10-fold reduction of single-channel conductance ($\sim$0.07 pS). The conductance of the F484C mutant was reduced to $\sim$0.2 pS (data not shown). This is consistent with F484 lining directly the pore. Of note, the equivalent residue to F484 coordinates Cl^- in the StClC crystal (Dutzler et al., 2002). Both mutations also changed ClC-1 gating, with F484A having stronger effects (Figures 8C and 8D). Both mutants remained anion selective with a preference of $Cl^- > Br^- > I^-$ similar to WT ClC-1 (data not shown).

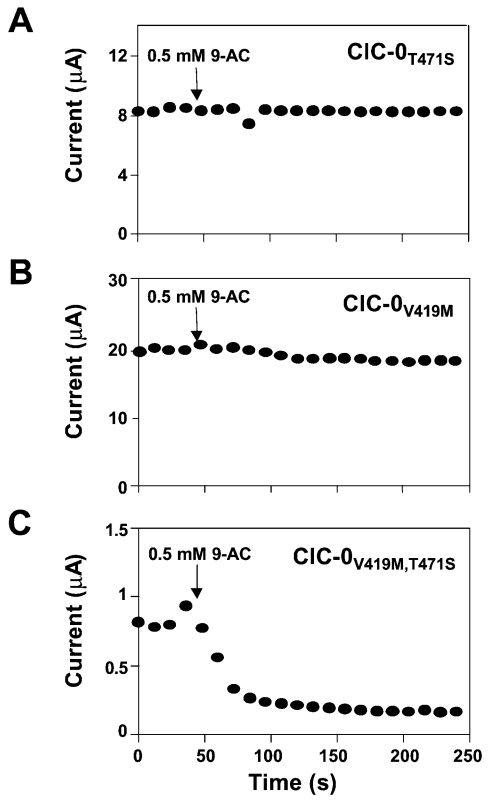

Figure 7. Reconstituting the 9-AC Binding Site in ClC-0 by a Double Mutation

(A) Superfusion with 0.5 mM 9-AC of an oocyte injected with the T471S mutant of ClC-0 does not result in current inhibition. The V419M mutant (B) is also resistant to 9-AC. (C) Introducing the double mutation T471S/V419M results in 9-AC sensitivity in an experiment done under otherwise identical conditions. Note that currents of the double mutant are typically much smaller. Oocytes were held at −30mV and stepped repeatedly every 12 s sequentially to +40mV and −140mV (pulse durations, 100 ms (+40mV) and 200 ms (−140mV), respectively; holding potential, −40mV). The current at +40mV is shown as a function of time. Similar effects were observed in four experiments. K_ds for 9-AC inhibition were above 1 mM for the single mutants and 107 ± 12 μM for $ClC\text{-}0_{V419M,T471S}$.

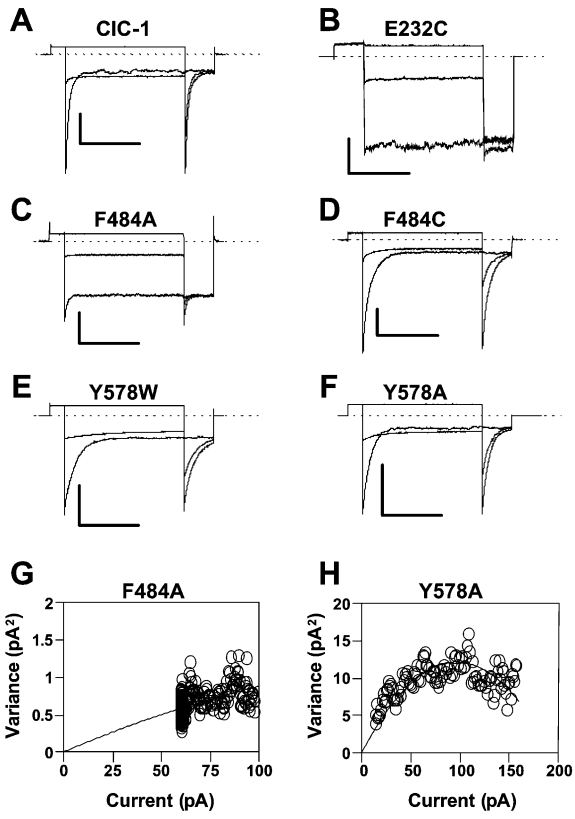

Figure 8. Biophysical Properties of ClC-1 Pore Mutants

(A–F) Inside-out patch clamp measurements of WT ClC-1 (A) and various point mutations affecting crucial amino acids (B–F). Patches were clamped between −140mV and +80mV for 400 ms in steps of 20mV, after a prepulse to +60mV and followed by a test pulse to −140mV. For clarity, only traces for −140mV, −60mV, and +60mV are shown. Horizontal scale bars indicate 200 ms, and vertical scale bars indicate 100 pA, WT ClC-1; 100 pA, E232C; 25 pA, F484A; 50 pA, F484C; 400 pA, Y578W; 200 pA, Y578A.

(G and H) Noise analysis of point mutants that change the Cl^- coordinating amino acids F484 and Y578. Nonstationary noise analysis of time-dependent currents observed upon stepping to −160mV was performed (Pusch et al., 1994). The variance of the current is plotted as a function of its magnitude. From these data, the single-channel conductance of $ClC\text{-}1_{F484A}$ is estimated to 0.07 ± 0.05 pS (SD, n = 7), that of $ClC\text{-}1_{Y578A}$ to 1.8 ± 0.4 pS (SD, n = 8), and that of $ClC\text{-}1_{Y578W}$ to 1.2 ± 0.2 (SD, n = 4) (data not shown), which compare to 1–2 pS for WT ClC-1 (Pusch et al., 1994; Saviane et al., 1999).

Mutations in Y578 (helix R) had comparatively minor effects on 9-AC inhibition, although the crystal structure suggests that both Y578 and F484 coordinate Cl^-. Noise analysis indicated that the single-channel conductance of Y578A amounted to 1.8 ± 0.4 pS and thus was not much different from WT (Figure 8H). $ClC\text{-}1_{Y578A}$ and $ClC\text{-}1_{Y578W}$ retained a $Cl^- > Br^- > I^-$ selectivity sequence, indicating that pore properties are largely conserved.

When E232 was mutated, the channel completely lost its voltage-dependent gating (Figure 8B for E232C). This finding agrees with the proposed role of this glutamate in gating. Its single-channel conductance as estimated by noise analysis in the presence of 20 μM CPA (to introduce current relaxations) was close to the WT value (1.3 ± 0.3 pS, data not shown). Similar to previously described E232Q and E232K mutants (Fahlke et al., 1997b), E232C and E232A also retained the WT $Cl^- > Br^- > I^-$ selectivity sequence.

Discussion

Despite the enormous physiological importance of Cl^- channels, their pharmacology is much less developed than that of cation channels (Jentsch et al., 2002). With the exception of drugs targeting ligand-gated $GABA_A$ and glycine receptor channels, Cl^- channel inhibitors have mostly low affinities, and it has remained unclear where they bind to the channel protein. In this work, we have identified an inhibitor binding site in a CLC channel.

Starting from a critical amino acid identified by a chimeric approach, we have used the bacterial structure to predict further amino acids that might be important for inhibitor binding. The fact that the side chains of

StClC amino acids that correspond to ClC-1 residues that strongly influence 9-AC block cluster around a rather well defined "pocket," lined by amino acids from different helices and loops, demonstrates that structures of CLC proteins are highly conserved.

9-AC Binds from the Intracellular Side

The crystal structure of the StClC protein (Dutzler et al., 2002) revealed that valine 402, the bacterial residue corresponding to ClC-1 S537 that was identified in our chimeric approach, is located deep in the channel protein. It is predicted to be accessible only from the intracellular side. This agrees with the sidedness of inhibitor action and its voltage-dependence. Indeed, CPA and related substances exert a strongly voltage-dependent block that is relieved at inside-positive voltages that tend to open the channel (Aromataris et al., 1999; Pusch et al., 2000, 2001). This observation is consistent with negatively charged CPA being driven into the pore from the cytoplasmic side at inside-negative voltages. Although 9-AC block was previously thought to be voltage independent, the present data show that it similarly depends on voltage. The main difference lies in its extremely slow binding/unbinding kinetics. When applied extracellularly in whole-cell measurements, the hydrophobic 9-AC molecule has to diffuse across the membrane to reach its site of action. Together with its slow binding kinetics, this explains the notoriously slow effect of 9-AC on ClC-1. The slower onset of inhibition (but unchanged affinity) observed with a charge reversal of K585, whose side chain probably protrudes into the intracellular entrance of the pore (Dutzler et al., 2002), is consistent with the hypothesis that 9-AC reaches its binding site through the same pathway that is used by Cl^- ions in the permeation process. However, as K585E also changes the gating of the channel, we cannot exclude that 9-AC reaches its binding site through some other pathway that is less frequently accessible in the K585E mutant.

The Inhibitor Binding Pocket in ClC-1

All high-impact amino acids that strongly affected channel block clustered in a region that is accessible from the cytoplasm and that partially overlaps with the Cl^- binding site in the bacterial protein (Dutzler et al., 2002). The high-impact residues are located in several different helices: the beginning of helix F (E232; based on CPA affinity), helix H (F288), beginning of helix N (F484 and neighbors), and the stretch between helix O and P (V536, S537, and H538). They surround a partially hydrophobic pocket that is large enough to accommodate either 9-AC or CPA (R.E. and T.J.J., unpublished data). The medium-impact amino acids, the mutations of which had moderate effects on channel inhibition, are located in the same region and are often directly adjacent to high-impact residues. The side chains of most high- and medium-impact residues point into the putative binding pocket. However, there are some exceptions. For instance, the side chains of the high-impact residues V487 and V536 do not point directly into the pocket in the ClC-1 structural model (Figure 6B), and the side chain of the medium-impact isoleucine 290 (which is mutated in a pedigree with dominant myotonia [Pusch et al., 1995b]) conspicuously points away from it (Figure 6C). Hence, the effects of these mutations may be due to conformational changes. In particular, mutations in V536 may influence the neighboring high-impact amino acid S537. On the other hand, residues pointing into the pocket (in particular the high-impact ones) are likely to interact more directly with the inhibitor.

By contrast, most amino acids that had little effect on channel block were at a larger distance from this pocket or had side chains that pointed away from it (blue residues in Figures 6B and 6C). This strongly argues that most of the observed pharmacological effects are specific and not due to overall conformational rearrangements in this highly conserved region.

In the binding pocket, the inhibitor may interact with several aromatic residues, i.e., with F484, and, possibly to a lesser degree, with F288. As both 9-AC and CPA are also aromatic compounds, this may involve hydrophobic or π stacking interactions as proposed for other drug-channel interactions (Mitcheson et al., 2000). The direct neighbors of F484 also influenced 9-AC block. G483 is classified as a high-impact residue and M485 as a medium-impact residue. Substitution of M485 by valine in ClC-0 abolished 9-AC sensitivity, while mutating it to cysteine in ClC-1 (M485C) increased 9-AC affinity. It is interesting to note that the more hydrophobic 9-AC is strongly influenced by mutations in both F288 and F484, whereas the efficacy of the less hydrophobic CPA depends much more on F288 than on F484 (Figure 5).

Two high-impact (G483, F484) and two medium-impact (S189, Y578) residues coordinate a Cl^- ion in the StClC crystal (Dutzler et al., 2002). Therefore, one may speculate that the negative side chain of either 9-AC or CPA may interact with these residues, possibly in competition with Cl^-. Inhibition by 9-AC was correlated with the side chain volume of the amino acid at position 537, which is occupied by serine in WT ClC-1. This residue is not expected to interact with the Cl^- as inferred from the StClC crystal. Substitutions with larger or smaller side chains decreased or increased 9-AC affinity, respectively. This may indicate a direct effect, or the orientation of another residue, which directly contacts 9-AC, may be dependent on the residue at this position.

9-AC and CPA Binding Have Different Structural Requirements

The S537T mutation in ClC-1 did not only affect the block by 9-AC but also caused about a 10-fold difference in affinity for CPA, a chemically quite different blocker. It was also possible to transfer CPA sensitivity to ClC-0 and ClC-2 by changing the corresponding threonines to serines. However, while the ClC-2 mutant was also sensitive to 9-AC, the ClC-0 mutant was resistant. This clearly shows that the binding sites for these inhibitors are overlapping but not identical. This is also supported by the differential effect of the present ClC-1 mutations on 9-AC and CPA block, respectively (Figure 5). By comparing sequences between ClC-0, -1, and -2 and taking into account the crystal structure, we identified a second residue (M485 in ClC-1) that is important for 9-AC- but not for CPA binding. Combining the two point mutations (T471S and V419M) that introduce ClC-1 residues at the

equivalent ClC-0 positions, we created a 9-AC binding site in ClC-0. The structural basis for the requirement of a methionine in ClC-0 at position 419 for the observed 9-AC sensitivity is, however, obscure, as the reverse mutation in ClC-1 (M485V) decreased 9-AC sensitivity only moderately. The side chain of the corresponding StClC residue A358 points toward the extracellular direction, toward E148, the glutamate that is implicated in gating. An indirect effect on 9-AC sensitivity can therefore not be excluded.

The StClC structure probably represents a closed channel (Dutzler et al., 2002). Hence, it is likely that we have identified the inhibitor binding site in the closed conformation. This is compatible with recent findings that clofibrates bind with higher affinity to the closed than to the open state of ClC-1 (Pusch et al., 2001). This in turn underlies the voltage-dependent block by CPA and possibly also by 9-AC.

Effect of Point Mutations on Pore Properties and Gating

The originally identified serine 537 is predicted to be at a relatively large distance of ~7 Å from the Cl^- binding site. Mutating this residue did not greatly alter open-pore properties like ion selectivity and single-channel conductance. Thus, S537 is probably not directly involved in forming the ion-selective pore.

In contrast, the crystal structure predicts that the ClC-1 residues S189, G483, F484, and Y578 may directly coordinate a Cl^- ion (Dutzler et al., 2002). Except for the glycine, these amino acids are extremely conserved among species and homologs, although, in a rare exception, the tyrosine is replaced by alanine in the yeast ScClC (Gef1p) (Greene et al., 1993). Mutations in F484 (F484A and F484C) indeed drastically reduced single-channel conductance but left the $Cl^- > Br^- > I^-$ selectivity sequence intact. We have shown previously that mutating the ClC-0 equivalent of ClC-1 S189 to threonine (S123T) reduced single-channel conductance and moderately changed halide selectivity (Ludewig et al., 1996). Somewhat surprisingly, no significant changes in single-channel conductances and halide selectivity sequences were observed with mutations in Y578 (Y578W and Y578A; Figures 8G and 8H). Interestingly, methionine 485 of ClC-1 that now turns out to influence 9-AC binding and that is a direct neighbor of Cl^- coordinating F484, is mutated to valine in a patient with recessive myotonia (Meyer-Kleine et al., 1995). The M485V mutation reduced single-channel conductance to ~0.3 pS (Wollnik et al., 1997).

Hence, mutating amino acids corresponding to Cl^--coordinating residues in the crystal of the bacterial protein (Dutzler et al., 2002) does not necessarily change pore properties such as single-channel conductance and ion selectivity. This is compatible with the notion that the published crystal structure shows a closed conformation of the channel. For K^+ channels, it was recently shown that open and closed configurations differ significantly (Jiang et al., 2002). Until the open conformation of CLC channels is known, it is unclear whether and to which extent the crystallographically resolved Cl^- binding site correlates with a selectivity filter. Thus, the negligible biophysical effects of mutating Y578 may indicate that in an open configuration this residue does not exert a large influence on the permeating anion.

Many mutations analyzed here also changed ClC-1 gating to varying degrees (Figure 8). Permeation and gating are tightly coupled in CLC channels (Pusch et al., 1995a), and many mutations in different parts of CLC proteins change gating (Fahlke et al., 1995, 1997b; Jentsch et al., 2002; Ludewig et al., 1997; Pusch et al., 1995b). Of particular interest are mutations in E232. In the crystal structure of the bacterial protein, its negatively charged side chain obstructs the pore above the Cl^- binding site. This led to the suggestion that this side chain may represent a gate (Dutzler et al., 2002) that possibly moves out of the permeation pathway in response to the presence of anions, thereby explaining Cl^--dependent gating (Pusch et al., 1995a). In agreement with this hypothesis, the E232C mutant almost totally lacked gating (Figure 8B). ClC-K channels, in which, in a rare exception, this glutamate is replaced by valine or leucine (Kieferle et al., 1994) have minimal gating (Estévez et al., 2001; Waldegger and Jentsch, 2000), and introducing glutamate at this position strongly enhanced and changed gating (Waldegger and Jentsch, 2000). Replacing the equivalent E to A in either ClC-4 or ClC-5 also seemed to abolish gating (Friedrich et al., 1999). On the other hand, mutations in E232 of ClC-1 did not change ion selectivity (Fahlke et al., 1997a) and single-channel conductance, in further agreement with this hypothesis.

Conclusion

In this work, we have identified and characterized an inhibitor binding site in a CLC chloride channel. It is localized close to the chloride binding site and is accessible only from the intracellular side. Exchanges of single amino acids have large differential effects on two classes of inhibitors. The successful use of the 3D crystal structure of the bacterial StClC protein to predict additional residues involved in inhibitor binding demonstrates that the structures of CLC channels are highly conserved between bacteria and mammals. Our results suggest that molecular modeling based on the bacterial channel may be useful to develop new drugs targeting specific channels of this ion channel class. The crucial role of CLC channels in cell physiology, as demonstrated by their mutational inactivation in several human diseases, makes them prime targets for synthetic drugs of medical importance.

Experimental Procedures

Construction of Mutant Channels and Expression in *Xenopus* Oocytes

Human ClC-1 and rat ClC-2 clones were used. Cloning of ClC-0, ClC-1, and ClC-2 into the oocyte expression vector PTLN was previously described (Lorenz et al., 1996; Ludewig et al., 1996). Chimeras and point mutants were constructed by recombinant PCR. Numbering in chimeras always represents amino acid positions from the complete channels the fragments were taken from (accession numbers: ClC-0, CAA40078; hClC-1: CAA80996; rClC-2: CAA45500). $ClC\text{-}1_{\leq 295}$; $ClC\text{-}2_{\geq 273;\leq 449}$; $ClC\text{-}1_{\geq 468}$ e.g., represents a chimera whose first 295 amino acids are from ClC-1, followed by amino acids 273 to 449 of ClC-2, followed by all ClC-1 amino acids after position 468. The amino acids 16 to 61 are deleted in the $ClC\text{-}2_{\Delta 16\text{-}61}$ mutant. For the patch clamp analysis of ClC-0 constructs, we additionally

inserted a point mutation that completely eliminates the slow gate (C212S) (Lin et al., 1999).

Capped cRNA was transcribed in vitro from constructs that were linearized with MluI using SP6 RNA polymerase in the mMessage mMachine kit (Ambion, Austin, TX). *Xenopus* oocytes were prepared by collagenase treatment, injected with 1–5 ng cRNA, and incubated at 17°C. Measurements were performed 2–4 days after injection.

Electrophysiology

Voltage clamp measurements were performed at room temperature using a two-electrode voltage clamp amplifier (Turbo Tec 10C, npi, Tamm, Germany) and pClamp software (Axon Instruments, Foster City, CA). Oocytes where continuously superfused by ND96 (96 mM NaCl, 2 mM KCl, 1.8 mM $CaCl_2$, 1 mM $MgCl_2$, 5 mM HEPES [pH 7.4]) containing 1% dimethylsulfoxide (DMSO) or solutions as indicated. At this concentration, DMSO had no obvious effect on currents. Solutions containing inhibitors were prepared freshly before application.

Patch clamp measurements (in the excised outside-out or inside-out mode) were performed after manual removal of the vitelline envelope. Patch pipettes of 1–5 MΩ resistance were pulled from aluminosilicate glass (Hilgenberg, Malsfeld, Germany), coated with Sylgard (General Electric, Waterford, NY), and filled with 100 mM NMDG-Cl, 5 mM $MgCl_2$, 5 mM HEPES (pH 7.4). The bath solution contained 106 mM NMDG-Cl, 2 mM $MgCl_2$, 2.5 mM EGTA, 5 mM HEPES (pH 7.4), resulting in a symmetrical Cl^- concentration of 110 mM. Data were acquired with an EPC-7 amplifier (HEKA, Lambrecht, Germany) and Pulse software (HEKA, Lambrecht, Germany).

Data Analysis

To determine 9-AC potency, current amplitudes where measured at the end of a 100 ms voltage step from a holding potential of −40mV to +60mV before (I_{max}) and 3–20 min after 9-AC treatment [I(c)] and fitted for each oocyte individually using SigmaPlot 4.0 Software (Jandel, San Rafael, CA) to the following function:

$$I(c) = (I_{max} - I_{min})/(1 + (c/K_d)) + I_{min}$$

c denotes the inhibitor concentration, K_d the apparent concentration of half maximal inhibition, and I_{min} the current remaining at saturating inhibitor concentration or in a solution in which NaCl was replaced by NaI, a condition that completely blocks ClC-1 (Rychkov et al., 1998). During the perfusion with 9-AC, the onset of block was monitored. Only experiments in which a reasonable steady state was reached were used for the calculation of the K_d. All mutants were practically completely blocked by I^- except V544W. The expression level of this mutant was, however, relatively low, and the apparent lack of the I^- effect was not investigated further. Amplitude measurements in voltage clamp experiments, after applying periodic test pulses indicated that a steady state was reached. However, for some mutants (e.g., K585E), the inhibitory effect did not fully reach steady state within a time that allowed meaningful measurements of currents (i.e., about 20 min). Apparent K_ds obtained under these conditions tend to overestimate the real K_d. Apparent K_d values are expressed as mean ± SEM.

Noise Analysis

Estimates for single-channel conductances were obtained by non-stationary noise analysis as described (Pusch et al., 2001). Briefly, about 100 pulses to a test potential of −160mV or −100mV were repetitively applied, and the mean response, I, was calculated. The variance, σ^2, was calculated from the averaged squared difference of consecutive traces. Background variance at 0mV was subtracted, and the variance-mean plot was fitted by $\sigma^2 = iI - I^2/N$, with the single-channel current, i, and the number of channels, N, as free parameters. The single-channel conductance was approximated assuming a linear i-V relationship.

Molecular Modeling

The coordinates of the StClC protein (Dutzler et al., 2002) were obtained from R. MacKinnon and were used as the template for a homology model created by the MODELER program within the InsightII interface (Vers. 2000, Accelrys, San Diego, CA). The sequence alignment from Dutzler et al. (2002) was used to create models for ClC-1 (112-596) dimers. The lowest energy model was selected.

Acknowledgments

We thank Janna Enderich, Sonia Traverso, and Laura Elia for technical assistance; and Rod MacKinnon for making the StClC coordinates available to us prior to publication. Supported by grants from Ministero Italiano Università Ricerca Italy (FIRB RBAU01PJMS) and Telethon Italy to M.P., and by grants from the Deutsche Forschungsgemeinschaft and the Prix Louis Jeantet de Médecine (to T.J.J.). R.E. is supported by a Marie Curie fellowship from the European Union.

Received: July 29, 2002
Revised: February 19, 2003
Accepted: March 14, 2003
Published: April 9, 2003

References

Aromataris, E.C., Astill, D.S., Rychkov, G.Y., Bryant, S.H., Bretag, A.H., and Roberts, M.L. (1999). Modulation of the gating of ClC-1 by S-(-) 2-(4-chlorophenoxy) propionic acid. Br. J. Pharmacol. *126*, 1375–1382.

Astill, D.S., Rychkov, G., Clarke, J.D., Hughes, B.P., Roberts, M.L., and Bretag, A.H. (1996). Characteristics of skeletal muscle chloride channel ClC-1 and point mutant R304E expressed in Sf9 insect cells. Biochim. Biophys. Acta *1280*, 178–186.

Bauer, C.K., Steinmeyer, K., Schwarz, J.R., and Jentsch, T.J. (1991). Completely functional double-barreled chloride channel expressed from a single *Torpedo* cDNA. Proc. Natl. Acad. Sci. USA *88*, 11052–11056.

Birkenhäger, R., Otto, E., Schürmann, M.J., Vollmer, M., Ruf, E.M., Maier-Lutz, I., Beekmann, F., Fekete, A., Omran, H., Feldmann, D., et al. (2001). Mutation of *BSND* causes Bartter syndrome with sensorineural deafness and kidney failure. Nat. Genet. *29*, 310–314.

Bösl, M.R., Stein, V., Hübner, C., Zdebik, A.A., Jordt, S.E., Mukhophadhyay, A.K., Davidoff, M.S., Holstein, A.F., and Jentsch, T.J. (2001). Male germ cells and photoreceptors, both depending on close cell-cell interactions, degenerate upon ClC-2 Cl^--channel disruption. EMBO J. *20*, 1289–1299.

Bryant, S.H., and Morales-Aguilera, A. (1971). Chloride conductance in normal and myotonic muscle fibres and the action of monocarboxylic aromatic acids. J. Physiol. *219*, 367–383.

Clark, S., Jordt, S.E., Jentsch, T.J., and Mathie, A. (1998). Characterization of the hyperpolarization-activated chloride current in dissociated rat sympathetic neurons. J. Physiol. *506*, 665–678.

Creighton, T.E. (1993). Proteins (New York: W.H. Freeman and Co.).

De Luca, A., Tricarico, D., Wagner, R., Bryant, S.H., Tortorella, V., and Conte Camerino, D. (1992). Opposite effects of enantiomers of clofibric acid derivative on rat skeletal muscle chloride conductance: antagonism studies and theoretical modeling of two different receptor site interactions. J. Pharmacol. Exp. Ther. *260*, 364–368.

Dutzler, R., Campbell, E.B., Cadene, M., Chait, B.T., and MacKinnon, R. (2002). X-ray structure of a ClC chloride channel at 3.0 A reveals the molecular basis of anion selectivity. Nature *415*, 287–294.

Estévez, R., and Jentsch, T.J. (2002). CLC chloride channels: correlating structure and function. Curr. Opin. Struct. Biol. *12*, 531–539.

Estévez, R., Boettger, T., Stein, V., Birkenhäger, R., Otto, M., Hildebrandt, F., and Jentsch, T.J. (2001). Barttin is a Cl^--channel β-subunit crucial for renal Cl^--reabsorption and inner ear K^+-secretion. Nature *414*, 558–561.

Fahlke, C., Rüdel, R., Mitrovic, N., Zhou, M., and George, A.L., Jr. (1995). An aspartic acid residue important for voltage-dependent gating of human muscle chloride channels. Neuron *15*, 463–472.

Fahlke, C., Knittle, T., Gurnett, C.A., Campbell, K.P., and George, A.L., Jr. (1997a). Subunit stoichiometry of human muscle chloride channels. J. Gen. Physiol. *109*, 93–104.

Fahlke, C., Yu, H.T., Beck, C.L., Rhodes, T.H., and George, A.L., Jr.

(1997b). Pore-forming segments in voltage-gated chloride channels. Nature *390*, 529–532.

Friedrich, T., Breiderhoff, T., and Jentsch, T.J. (1999). Mutational analysis demonstrates that ClC-4 and ClC-5 directly mediate plasma membrane currents. J. Biol. Chem. *274*, 896–902.

Greene, J.R., Brown, N.H., DiDomenico, B.J., Kaplan, J., and Eide, D.J. (1993). The *GEF1* gene of *Saccharomyces cerevisiae* encodes an integral membrane protein; mutations in which have effects on respiration and iron-limited growth. Mol. Gen. Genet. *241*, 542–553.

Gründer, S., Thiemann, A., Pusch, M., and Jentsch, T.J. (1992). Regions involved in the opening of ClC-2 chloride channel by voltage and cell volume. Nature *360*, 759–762.

Günther, W., Lüchow, A., Cluzeaud, F., Vandewalle, A., and Jentsch, T.J. (1998). ClC-5, the chloride channel mutated in Dent's disease, colocalizes with the proton pump in endocytotically active kidney cells. Proc. Natl. Acad. Sci. USA *95*, 8075–8080.

Hille, B. (2001). Ion Channels of Excitable Membranes, Third edition (Sunderland, MA: Sinauer Associates).

Jentsch, T.J., Steinmeyer, K., and Schwarz, G. (1990). Primary structure of *Torpedo marmorata* chloride channel isolated by expression cloning in *Xenopus* oocytes. Nature *348*, 510–514.

Jentsch, T.J., Stein, V., Weinreich, F., and Zdebik, A.A. (2002). Molecular structure and physiological function of chloride channels. Physiol. Rev. *82*, 503–568.

Jiang, Y., Lee, A., Chen, J., Cadene, M., Chait, B.T., and MacKinnon, R. (2002). The open pore conformation of potassium channels. Nature *417*, 523–526.

Kieferle, S., Fong, P., Bens, M., Vandewalle, A., and Jentsch, T.J. (1994). Two highly homologous members of the ClC chloride channel family in both rat and human kidney. Proc. Natl. Acad. Sci. USA *91*, 6943–6947.

Koch, M.C., Steinmeyer, K., Lorenz, C., Ricker, K., Wolf, F., Otto, M., Zoll, B., Lehmann-Horn, F., Grzeschik, K.H., and Jentsch, T.J. (1992). The skeletal muscle chloride channel in dominant and recessive human myotonia. Science *257*, 797–800.

Kornak, U., Kasper, D., Bösl, M.R., Kaiser, E., Schweizer, M., Schulz, A., Friedrich, W., Delling, G., and Jentsch, T.J. (2001). Loss of the ClC-7 chloride channel leads to osteopetrosis in mice and man. Cell *104*, 205–215.

Langer, T., and Levy, R.I. (1968). Acute muscular syndrome associated with administration of clofibrate. N. Engl. J. Med. *279*, 856–858.

Lin, Y.W., Lin, C.W., and Chen, T.Y. (1999). Elimination of the slow gating of ClC-0 chloride channel by a point mutation. J. Gen. Physiol. *114*, 1–12.

Lloyd, S.E., Pearce, S.H., Fisher, S.E., Steinmeyer, K., Schwappach, B., Scheinman, S.J., Harding, B., Bolino, A., Devoto, M., Goodyer, P., et al. (1996). A common molecular basis for three inherited kidney stone diseases. Nature *379*, 445–449.

Lorenz, C., Pusch, M., and Jentsch, T.J. (1996). Heteromultimeric CLC chloride channels with novel properties. Proc. Natl. Acad. Sci. USA *93*, 13362–13366.

Ludewig, U., Pusch, M., and Jentsch, T.J. (1996). Two physically distinct pores in the dimeric ClC-0 chloride channel. Nature *383*, 340–343.

Ludewig, U., Jentsch, T.J., and Pusch, M. (1997). Inward rectification in ClC-0 chloride channels caused by mutations in several protein regions. J. Gen. Physiol. *110*, 165–171.

Matsumura, Y., Uchida, S., Kondo, Y., Miyazaki, H., Ko, S.B., Hayama, A., Morimoto, T., Liu, W., Arisawa, M., Sasaki, S., and Marumo, F. (1999). Overt nephrogenic diabetes insipidus in mice lacking the CLC-K1 chloride channel. Nat. Genet. *21*, 95–98.

Meyer-Kleine, C., Steinmeyer, K., Ricker, K., Jentsch, T.J., and Koch, M.C. (1995). Spectrum of mutations in the major human skeletal muscle chloride channel gene (*CLCN1*) leading to myotonia. Am. J. Hum. Genet. *57*, 1325–1334.

Middleton, R.E., Pheasant, D.J., and Miller, C. (1996). Homodimeric architecture of a ClC-type chloride ion channel. Nature *383*, 337–340.

Miller, C., and White, M.M. (1984). Dimeric structure of single chloride channels from Torpedo electroplax. Proc. Natl. Acad. Sci. USA *81*, 2772–2775.

Mitcheson, J.S., Chen, J., Lin, M., Culberson, C., and Sanguinetti, M.C. (2000). A structural basis for drug-induced long QT syndrome. Proc. Natl. Acad. Sci. USA *97*, 12329–12333.

Palade, P.T., and Barchi, R.L. (1977). On the inhibition of muscle membrane chloride conductance by aromatic carboxylic acids. J. Gen. Physiol. *69*, 879–896.

Pusch, M., Steinmeyer, K., and Jentsch, T.J. (1994). Low single channel conductance of the major skeletal muscle chloride channel, ClC-1. Biophys. J. *66*, 149–152.

Pusch, M., Ludewig, U., Rehfeldt, A., and Jentsch, T.J. (1995a). Gating of the voltage-dependent chloride channel ClC-0 by the permeant anion. Nature *373*, 527–531.

Pusch, M., Steinmeyer, K., Koch, M.C., and Jentsch, T.J. (1995b). Mutations in dominant human myotonia congenita drastically alter the voltage dependence of the ClC-1 chloride channel. Neuron *15*, 1455–1463.

Pusch, M., Jordt, S.E., Stein, V., and Jentsch, T.J. (1999). Chloride dependence of hyperpolarization-activated chloride channel gates. J. Physiol. *515*, 341–353.

Pusch, M., Liantonio, A., Bertorello, L., Accardi, A., De Luca, A., Pierno, S., Tortorella, V., and Camerino, D.C. (2000). Pharmacological characterization of chloride channels belonging to the ClC family by the use of chiral clofibric acid derivatives. Mol. Pharmacol. *58*, 498–507.

Pusch, M., Accardi, A., Liantonio, A., Ferrera, L., De Luca, A., Camerino, D.C., and Conti, F. (2001). Mechanism of block of single protopores of the *Torpedo* chloride channel ClC-0 by 2-(p-chlorophenoxy)butyric acid (CPB). J. Gen. Physiol. *118*, 45–62.

Rychkov, G.Y., Pusch, M., Roberts, M.L., Jentsch, T.J., and Bretag, A.H. (1998). Permeation and block of the skeletal muscle chloride channel, ClC-1, by foreign anions. J. Gen. Physiol. *111*, 653–665.

Saviane, C., Conti, F., and Pusch, M. (1999). The muscle chloride channel ClC-1 has a double-barreled appearance that is differentially affected in dominant and recessive myotonia. J. Gen. Physiol. *113*, 457–468.

Simon, D.B., Bindra, R.S., Mansfield, T.A., Nelson-Williams, C., Mendonca, E., Stone, R., Schurman, S., Nayir, A., Alpay, H., Bakkaloglu, A., et al. (1997). Mutations in the chloride channel gene, *CLCNKB*, cause Bartter's syndrome type III. Nat. Genet. *17*, 171–178.

Steinmeyer, K., Ortland, C., and Jentsch, T.J. (1991). Primary structure and functional expression of a developmentally regulated skeletal muscle chloride channel. Nature *354*, 301–304.

Steinmeyer, K., Schwappach, B., Bens, M., Vandewalle, A., and Jentsch, T.J. (1995). Cloning and functional expression of rat CLC-5, a chloride channel related to kidney disease. J. Biol. Chem. *270*, 31172–31177.

Stobrawa, S.M., Breiderhoff, T., Takamori, S., Engel, D., Schweizer, M., Zdebik, A.A., Bösl, M.R., Ruether, K., Jahn, H., Draguhn, A., et al. (2001). Disruption of ClC-3, a chloride channel expressed on synaptic vesicles, leads to a loss of the hippocampus. Neuron *29*, 185–196.

Varela, D., Niemeyer, M.I., Cid, L.P., and Sepulveda, F.V. (2002). Effect of an N-terminus deletion on voltage-dependent gating of the ClC- 2 chloride channel. J. Physiol. *544*, 363–372.

Waldegger, S., and Jentsch, T.J. (2000). Functional and structural analysis of ClC-K chloride channels involved in renal disease. J. Biol. Chem. *275*, 24527–24533.

Weinreich, F., and Jentsch, T.J. (2001). Pores formed by single subunits in mixed dimers of different CLC chloride channels. J. Biol. Chem. *276*, 2347–2353.

Wollnik, B., Kubisch, C., Steinmeyer, K., and Pusch, M. (1997). Identification of functionally important regions of the muscular chloride channel ClC-1 by analysis of recessive and dominant myotonic mutations. Hum. Mol. Genet. *6*, 805–811.